Issue Article

SOI: 1.1/TAS DOI: 10.15863/TAS

International Scientific Journal

**Theoretical & Applied Science**

**p-ISSN:** 2308-4944 (print) **e-ISSN:** 2409-0085 (online)

**Year:** 2026 **Issue:** 03 **Volume:** 155

**Received:** 24.03.2026
**Accepted/Published:** 30.03.2026

https://T-Science.org


**Denis Chemezov**
Vladimir Polytechnic College
MEng, Honorary Worker of the Education Field of the Russian Federation, Academician of International Academy of Theoretical and Applied Sciences, Lecturer, Russian Federation
https://orcid.org/0000-0002-2747-552X
vpk-science@yandex.ru

**Kirill Samokhvalov**
Vladimir Polytechnic College
Student, Russian Federation

**Yaroslav Baranov**
Vladimir Polytechnic College
Student, Russian Federation

**Aleksandr Burkov**
Vladimir Polytechnic College
Student, Russian Federation

**Darya Mishakova**
Vladimir Polytechnic College
Student, Russian Federation

**Valeriy Gogulin**
Vladimir Polytechnic College
Student, Russian Federation

**Ekaterina Suslova**
Vladimir Polytechnic College
Student, Russian Federation

**Daniil Firsov**
Vladimir Polytechnic College
Student, Russian Federation

**Andrey Stepanov**
Vladimir Polytechnic College
Student, Russian Federation


# ANALYSIS OF THE STRESS INTENSITY OF A PREHEATED STEEL BUSHING UNDER CONDITIONS OF PRESSING A STEEL SHAFT INTO IT TO FORM A FIT WITH A GUARANTEED INTERFERENCE

***Abstract***: *This article presents the results of finite element modeling of the process of pressing a shaft into a preheated bushing to form a fit with a guaranteed interference (0.1 mm). The intensity of the stress state of the bushing* *material was estimated based on the calculated values of von Mises stress, normal stress, and contact forces arising on the surfaces of the shaft and bushing.*

***Key words***: *bushing model, shaft model, pressing, stress, contact force.*

***Language***: *English*

***Citation***: Chemezov, D., et al. (2026). Analysis of the stress intensity of a preheated steel bushing under conditions of pressing a steel shaft into it to form a fit with a guaranteed interference. *ISJ Theoretical & Applied Science, 03 (155),* 215-220.

***Soi***: https://s-o-i.org/1.1/TAS-03-155-14 ***Doi***: crossref https://dx.doi.org/10.15863/TAS.2026.03.155.14

***Scopus ASCC***: *2206.*

## 1. Introduction

When pressing a steel shaft into a preheated steel bushing, the stress behavior within the materials is crucial to ensure a guaranteed interference fit. Heating the bushing causes it to expand, temporarily increasing the internal diameter. When cooled after assembly, the inner surface compresses tightly around the shaft, creating a strong mechanical connection without additional fastening.

The stress distribution during this process depends on temperature gradients, material properties and the amount of interference – the difference between the shaft diameter and the bushing bore [1-4]. Initially, thermal expansion reduces the pressing force, but as the bushing material cools, compressive hoop stresses arise, ensuring a secure fit [5-7]. In this case, the shaft experiences tensile stress due to compression.

Elastic deformation predominates during pressing, which turns into plastic deformation if the von Mises stress exceeds the yield strength of the material. Experimental and calculated data show that maximum von Mises stresses typically reach 85-110% of the yield strength for a successful interference fit [8-10].

Understanding the stress dynamics during shaft press-fitting is vital to predicting mechanical performance, preventing distortion, and ensuring reliability in applications such as mechanical engineering, automotive, and aerospace components where precision fit is critical.

## 2. Materials and methods

Finite element modeling of the process of pressing a shaft into a bushing was performed in the COMSOL Multiphysics software environment. Models of the bushing and shaft (the length of which was taken as 100 mm) were constructed on a plane. The difference between the outer diameter of the shaft model and the inner diameter of the bushing model was 0.1 mm, which made it possible to obtain the fit with guaranteed interference. The wall thickness of the bushing model was taken to be 15 mm. For more precise centering of the mating part models, two chamfers measuring 0.5×45° were made on their edges. The bushing model was fixed by the lower end surface, the shaft model moved only in the direction of the *Y* coordinate axis.

The conditions for finite element modeling of the process of pressing the shaft model into the bushing model are shown in the Fig. 1.

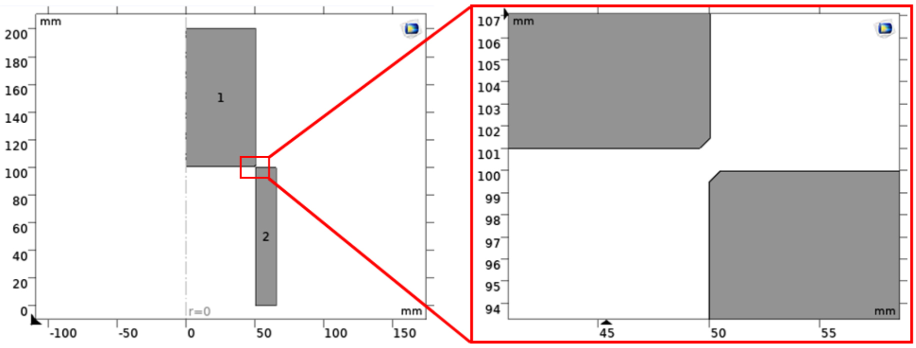


**Figure 1. The conditions for finite element modeling of the process of pressing the shaft model into the bushing model. The diagram shows: *1* – shaft model, *2* – bushing model, *r = 0* – center line of the shaft and bushing models.**

The bushing and shaft models were given the properties of 1040 steel, which has the properties of a linear elastic material. To facilitate the pressing process, the shaft model was cooled to a temperature of 123.15 K, and the bushing model was heated to a temperature of 473.15 K. The change in the mechanical properties of 1040 steel (Poisson's ratio, Young's modulus, bulk modulus and shear modulus) during heating and cooling is shown in the Fig. 2.

From the graphs it can be noted that when 1040 steel is cooled to extreme negative temperatures, the value of Poisson's ratio decreases, while the values of Young's modulus, bulk modulus and shear modulus increase. On the contrary, when heating 1040 steel, an increase in the Poisson's ratio and a decrease in the strength properties of the material are observed.

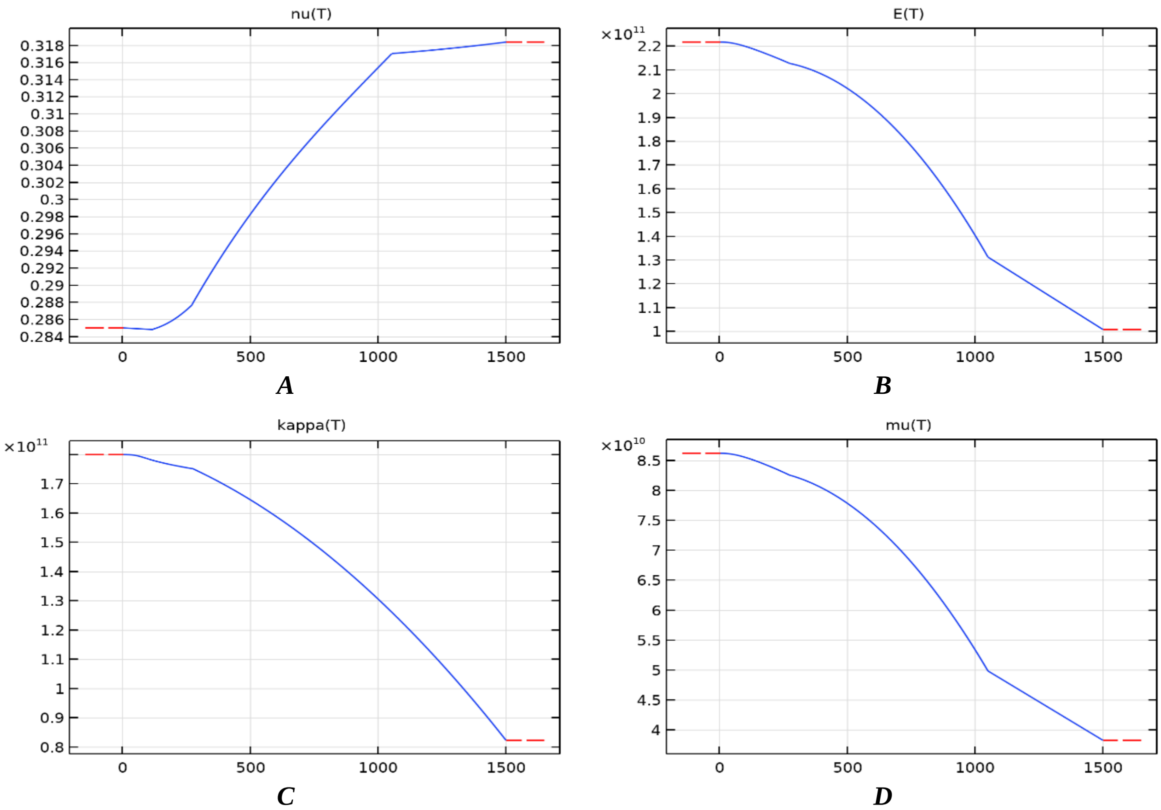


**Figure 2. Dependencies of mechanical properties of 1040 steel with temperature changes (K):**
***A* – Poisson's ratio, *B* – Young's modulus, *C* – bulk modulus and *D* – shear modulus.**

The contact of surfaces of the shaft and bushing models was determined using a friction coefficient of 0.5. The results of the stress state of the bushing material were recorded every 10 mm of the pressing length. The simulation was performed until the shaft model was completely pressed into the bushing model.

**3. Results and discussion**

The Table 1 shows the results of finite element modeling of the process of pressing the shaft model into the bushing model.

The results are presented in the form of a color scheme of the change in von Mises stress in the material of the bushing model, color vectors of contact forces on the mating surfaces of the shaft and bushing models, and the graphs of the dependence of normal stress of the contact inner surface of the bushing model on the pressing length.

The yield strength of 1040 steel is $3.35\times10^{8}$ N/m$^2$. At all steps of the calculation of the pressing process, an excess of the yield strength of the bushing material on the surface layers of the inner surface is observed, according to the calculated values of von Mises stress. In this case, the maximum stresses leading to plastic deformations are noted at a pressing length of 50 mm, and the minimum stresses are noted at a pressing length of 30 mm.

The pressing process is accompanied by the emergence of contact forces both on the outer surface of the shaft model and on the inner surface of the bushing model. The intensity of change in contact forces is shown by vectors of different lengths. The upper scale (with a color range from green to gray) shows the change in pressure on the contact surfaces of models, the lower scale (purple) shows the change in friction force on the contact surfaces of models. The friction force is constant in magnitude over the entire range of pressing length. It is noted that in the zone of cutting layers of material by the entry part of the shaft model, the greatest contact force acts on the inner surface of the bushing model. As the shaft model moves along the pressed length of the connection, a practically uniform distribution of force is observed on the contact surfaces of the part models. In this case, the material of the bushing model is subjected to compression, and the material of the shaft model is subjected to stretching. The greatest contact force occurs on the inner surface of the bushing model at a pressing length of 100 mm.

The graphs of the dependence of normal stress on the pressing length show the intensity of compression and tensile of the material of the bushing model in the mating zone. A zero value of normal stress characterizes the undeformed state of the material, positive values characterize the tensile of the material, and negative values characterize the compression of the material. Thus, the pressing mechanism can be represented as a compression zone at the mating of the shaft and bushing models; at a distance of up to 20 mm from the mating part, a tensile zone of the bushing model material arises, which transitions to a zone of undeformed state. At a pressing length of over 80 mm, a stick-slip effect is observed (the curve has a stick-slip oscillation), which may be caused by self-oscillations leading to a defective connection with interference fit.

**Table 1. Results of finite element modeling of the process of pressing the shaft model into the bushing model: the first column is the von Mises stress distribution in the bushing model; the second column is vectors of contact forces on the surfaces of the shaft and bushing models (green scale is pressure, purple scale is friction force); the third column is the dependence of normal stress on the inner surface of the bushing model on the pressing length.**

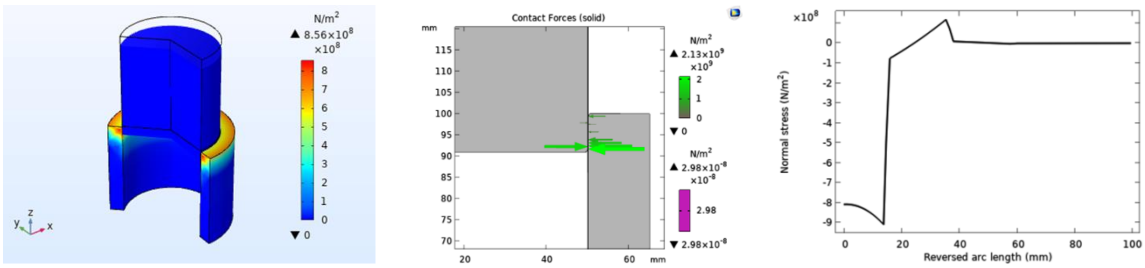


*Pressing length is 10 mm*

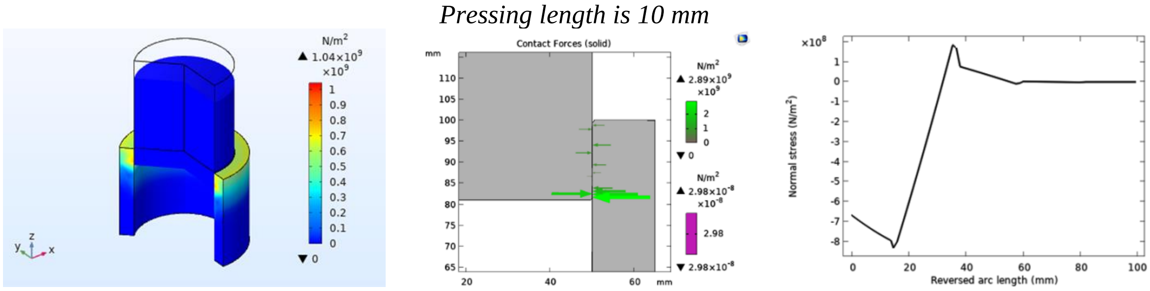


*Pressing length is 20 mm*

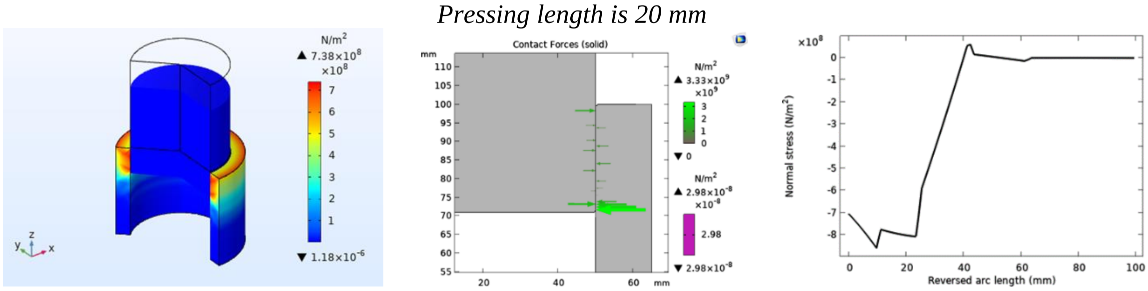


*Pressing length is 30 mm*

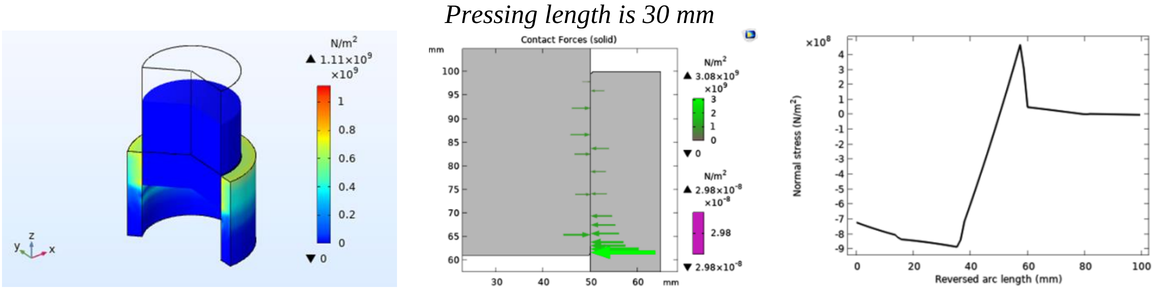


*Pressing length is 40 mm*

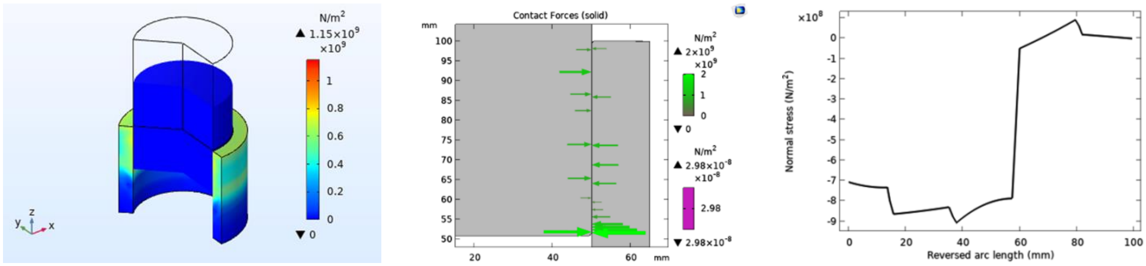


*Pressing length is 50 mm*

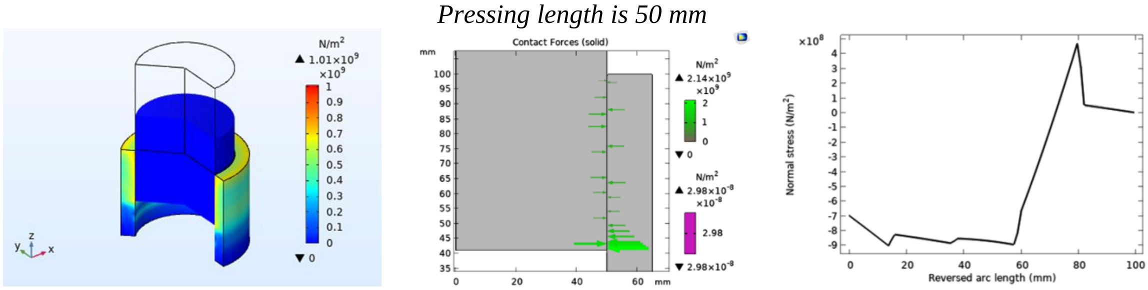


*Pressing length is 60 mm*

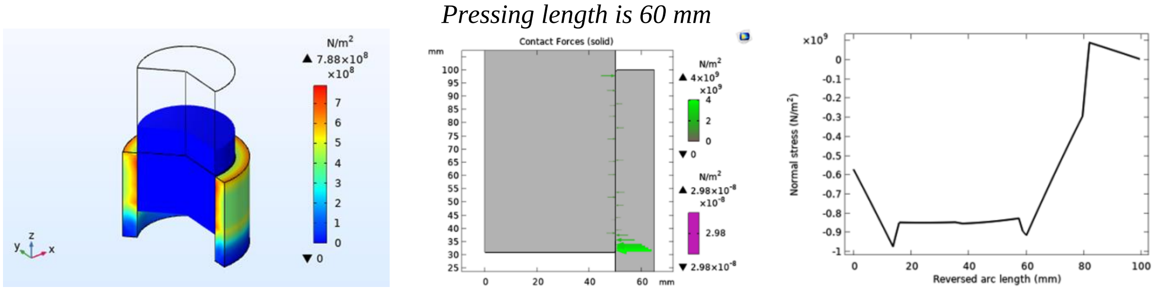


*Pressing length is 70 mm*

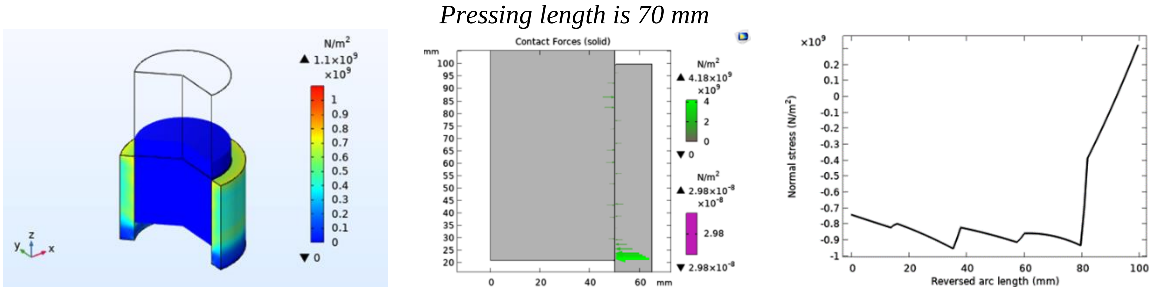


*Pressing length is 80 mm*

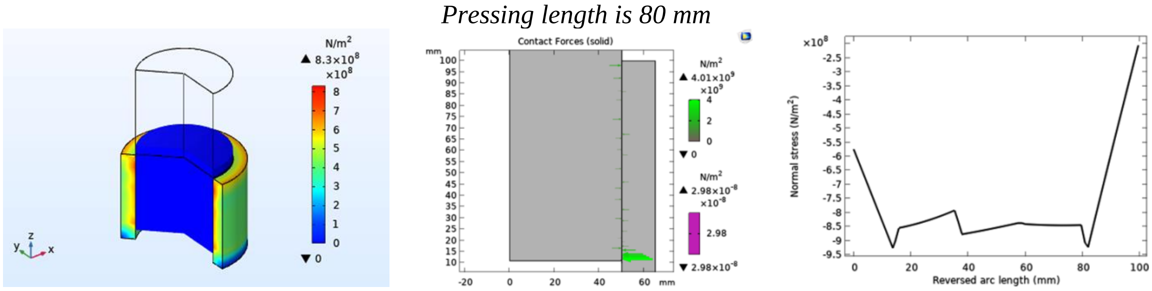


*Pressing length is 90 mm*

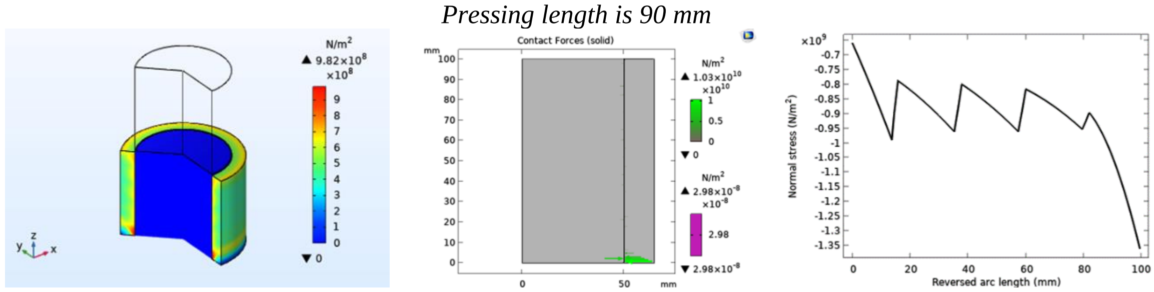


*Pressing length is 100 mm*

**4. Conclusion**

Thus, based on the analysis of the results of finite element modeling of the process of pressing the shaft into the bushing, with the formation of a guaranteed interference, the following conclusions can be drawn:

1. Over the entire length of the pressing, a "metal flow" effect occurs on the contact surface of the bushing, since the yield strength is exceeded more than twice for the selected material, in accordance with the von Mises stress criterion. The bushing material is subject to greater stress during the first half of the pressing length.

2. The contact force during the pressing process is maximum in the zone where the layers of material are cut by the entry part of the shaft. In this case, significant contact forces arise in the bushing material. Contact forces on the surface of the bushing lead to compression of the material, and on the surface of the shaft lead to stretching of the material. The greatest contact force occurs on the inner surface of the bushing at a pressing length of 100 mm.

3. The bushing material is subject to compression, which is confirmed by the dependence of normal stress (negative values) on the pressing length. At a pressing length of 100 mm, a clear stick-slip effect is observed (the curve has a stick-slip oscillation), which may be caused by damage to the contact surfaces of parts or unstable strength of the connection.

**References:**

1. Chemezov, D., et al. (2026). Forecast of strain intensity of a thin-walled steel bushing at a pressing length of up to 100 mm with guaranteed interference. *ISJ Theoretical & Applied Science, 02 (154)*, 75-84.
2. Shtern, M. B., Radomysel'skii, I. D., Pechentkovskii, E. L., Serdyuk, G. G., & Maksimenko, L. A. (1978). Effect of mode of pressing on the stressed-strained state of bushing-type parts. *Institute of Materials Science, Academy of Sciences of the Ukrainian SSR, T. G. Shevchenko Kiev State University, Translated from Poroshkovaya Metallurgiya, No. 3(183)*, 1-7.
3. Croccolo, D. De, Agostinis, M., & Vincenzi, N. (2010). Static and dynamic strength evaluation of interference fit and adhesively bonded cylindrical joints. *Int J Adhes, 30*, 359-366.
4. Pershin, V. F., & Selivanov, Yu. T. (2002). Calculation of the strength of thin-walled shells of revolution and thick-walled cylinders. *Tambov, GTU*, 20 p.
5. Yang, G. M., Coquille, J. C., Fontaine, J. F., & Lambertin, M. (2002). Contact pressure between two rough surfaces of cylindrical fit. *J Mater Process Technol*, *123*, 490-497.
6. Ryazantseva, I. L. (2018). Contact pressure with guaranteed tight in coupling of bushing and long shaft. *Omsk Scientific Bulletin. Series Aviation-Rocket and Power Engineering, Vol. 2, no. 4*, 15-20.
7. Seifi, R., Abbasi, K., & Asayesh, M. (2018). Effects of Contact Surface Roughness of Interference Shaft/Bush Joints on its Characteristics. *Iran J Sci Technol Trans Mech Eng, 42*, 279-292.
8. Boutoutaou, H., Bouazi, M., & Fontaine, J. F. (2011). Modeling of interference fits taking form defects of the surfaces in contact into account. *Mater Des, 32*, 3692-3701.
9. Ozel, A., Temiz, E., Aydin, M. D., & Sen, S. (2005). Stress analysis of shrink-fitted joints for various fit forms via finite element method. *J Mater Des, 26*, 281-289.
10. Seifi, R., & Abbasi, K. (2015). Friction coefficient estimation in shaft/bush interference using finite element model updating. *Eng Fail Anal, 57*, 310-322.